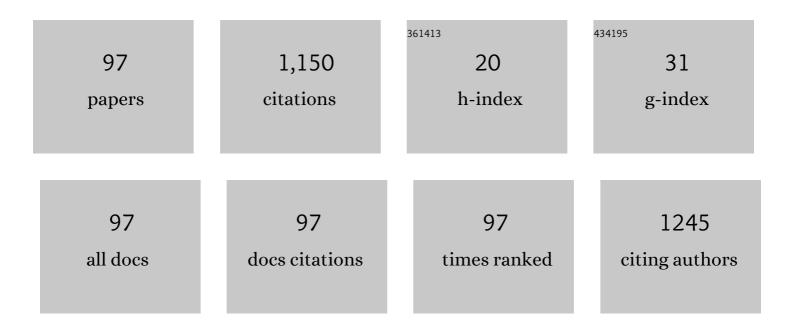
List of Publications by Year in descending order

Source: https://exaly.com/author-pdf/5661880/publications.pdf Version: 2024-02-01



CHIA-MING YANG

#	Article	IF	CITATIONS
1	Bidirectional Allâ€Optical Synapses Based on a 2D Bi ₂ O ₂ Se/Graphene Hybrid Structure for Multifunctional Optoelectronics. Advanced Functional Materials, 2020, 30, 2001598.	14.9	123
2	pH Sensitivity Improvement on 8 nm Thick Hafnium Oxide by Post Deposition Annealing. Electrochemical and Solid-State Letters, 2006, 9, G90.	2.2	78
3	pH sensing reliability of flexible ITO/PET electrodes on EGFETs prepared by a roll-to-roll process. Microelectronics Reliability, 2012, 52, 1651-1654.	1.7	54
4	Drift and Hysteresis Effects Improved by RTA Treatment on Hafnium Oxide in pH-Sensitive Applications. Journal of the Electrochemical Society, 2008, 155, J326.	2.9	38
5	Ultraviolet illumination effect on monolayer graphene-based resistive sensor for acetone detection. Vacuum, 2017, 140, 89-95.	3.5	38
6	N-Doped Graphene with Low Intrinsic Defect Densities via a Solid Source Doping Technique. Nanomaterials, 2017, 7, 302.	4.1	37
7	Enhanced acetone sensing properties of monolayer graphene at room temperature by electrode spacing effect and UV illumination. Sensors and Actuators B: Chemical, 2017, 253, 77-84.	7.8	36
8	Optimization of Urea-EnFET Based on Ta2O5 Layer with Post Annealing. Sensors, 2011, 11, 4562-4571.	3.8	34
9	Body effect minimization using single layer structure for pH-ISFET applications. Sensors and Actuators B: Chemical, 2010, 143, 494-499.	7.8	30
10	Sensing and pH-imaging properties of niobium oxide prepared by rapid thermal annealing for electrolyte–insulator–semiconductor structure and light-addressable potentiometric sensor. Sensors and Actuators B: Chemical, 2015, 207, 858-864.	7.8	30
11	Annealing effect on UV-illuminated recovery in gas response of graphene-based NO ₂ sensors. RSC Advances, 2019, 9, 23343-23351.	3.6	30
12	Low cost and flexible electrodes with NH3 plasma treatments in extended gate field effect transistors for urea detection. Sensors and Actuators B: Chemical, 2013, 187, 274-279.	7.8	28
13	Thickness Effects on pH Response of HfO2Sensing Dielectric Improved by Rapid Thermal Annealing. Japanese Journal of Applied Physics, 2006, 45, 3807-3810.	1.5	27
14	A high-speed, flexible-scanning chemical imaging system using a light-addressable potentiometric sensor integrated with an analog micromirror. Sensors and Actuators B: Chemical, 2014, 198, 225-232.	7.8	27
15	Speckled ZnO Nanograss Electrochemical Sensor for <i>Staphylococcus epidermidis</i> Detection. Journal of the Electrochemical Society, 2017, 164, B205-B211.	2.9	27
16	LAPS with nanoscaled and highly polarized HfO2 by CF4 plasma for NH4+ detection. Sensors and Actuators B: Chemical, 2013, 180, 71-76.	7.8	24
17	Suppression of Row Hammer Effect by Doping Profile Modification in Saddle-Fin Array Devices for Sub-30-nm DRAM Technology. IEEE Transactions on Device and Materials Reliability, 2016, 16, 685-687.	2.0	23
18	Non-ideal effects improvement of SF6 plasma treated hafnium oxide film based on electrolyte–insulator–semiconductor structure for pH-sensor application. Microelectronics Reliability, 2010, 50, 742-746.	1.7	20

#	Article	IF	CITATIONS
19	IGZO Thin-Film Light-Addressable Potentiometric Sensor. IEEE Electron Device Letters, 2016, 37, 1481-1484.	3.9	20
20	A Colloidal Nanopatterning and Downscaling of a Highly Periodic Au Nanoporous EGFET Biosensor. Journal of the Electrochemical Society, 2018, 165, H3170-H3177.	2.9	20
21	Characterization of K+ and Na+-Sensitive Membrane Fabricated by CF4 Plasma Treatment on Hafnium Oxide Thin Films on ISFET. Journal of the Electrochemical Society, 2011, 158, J91.	2.9	19
22	The physical and electrical characterizations of Cr-doped BiFeO3 ferroelectric thin films for nonvolatile memory applications. Microelectronic Engineering, 2015, 138, 86-90.	2.4	19
23	Plasmonic nanomaterial structuring for SERS enhancement. RSC Advances, 2019, 9, 4982-4992.	3.6	19
24	New pH-sensitive TaOxNy membranes prepared by NH3 plasma surface treatment and nitrogen incorporated reactive sputtering. Sensors and Actuators B: Chemical, 2008, 130, 77-81.	7.8	18
25	Immobilization of enzyme and antibody on ALD-HfO2-EIS structure by NH3 plasma treatment. Nanoscale Research Letters, 2012, 7, 179.	5.7	18
26	Characteristics of graphene grown through low power capacitive coupled radio frequency plasma enhanced chemical vapor deposition. Carbon, 2020, 159, 570-578.	10.3	18
27	P-I-N amorphous silicon for thin-film light-addressable potentiometric sensors. Sensors and Actuators B: Chemical, 2016, 236, 1005-1010.	7.8	17
28	Spatial resolution and 2D chemical image of light-addressable potentiometric sensor improved by inductively coupled-plasma reactive-ion etching. Sensors and Actuators B: Chemical, 2018, 258, 1295-1301.	7.8	17
29	Hysteresis effect on traps of Si3N4 sensing membranes for pH difference sensitivity. Microelectronics Reliability, 2010, 50, 738-741.	1.7	16
30	Analog micromirror-LAPS for chemical imaging and zoom-in application. Vacuum, 2015, 118, 161-166.	3.5	15
31	Surface Modification for High Photocurrent and pH Sensitivity in a Silicon-Based Light-Addressable Potentiometric Sensor. IEEE Sensors Journal, 2018, 18, 2253-2259.	4.7	12
32	Hydrogen ion sensing characteristics of IGZO/Si electrode in EGFET. International Journal of Nanotechnology, 2014, 11, 15.	0.2	11
33	Flexible Textile-Based Pressure Sensing System Applied in the Operating Room for Pressure Injury Monitoring of Cardiac Operation Patients. Sensors, 2020, 20, 4619.	3.8	11
34	A real-time mirror-LAPS mini system for dynamic chemical imaging and cell acidification monitoring. Sensors and Actuators B: Chemical, 2021, 341, 130003.	7.8	11
35	Light Addressable Potentiometric Sensor with Fluorine-Terminated Hafnium Oxide Layer for Sodium Detection. Japanese Journal of Applied Physics, 2010, 49, 04DL05.	1.5	10
36	Detection of KRAS mutation by combination of polymerase chain reaction (PCR) and EIS sensor with new amino group functionalization. Sensors and Actuators B: Chemical, 2013, 186, 374-379.	7.8	10

#	Article	IF	CITATIONS
37	A revised manuscript submitted to sensors and actuators B: Chemical illumination modification from an LED to a laser to improve the spatial resolution of IGZO thin film light-addressable potentiometric sensors in pH detections. Sensors and Actuators B: Chemical, 2021, 329, 128953.	7.8	10
38	Photoelectrochemical Detection of <i>β</i> -amyloid Peptides by a TiO ₂ Nanobrush Biosensor. IEEE Sensors Journal, 2020, 20, 6248-6255.	4.7	9
39	Superior Improvements in GIDL and Retention by Fluorine Implantation in Saddle-Fin Array Devices for Sub-40-nm DRAM Technology. IEEE Electron Device Letters, 2013, 34, 1124-1126.	3.9	8
40	Characterization on pH sensing performance and structural properties of gadolinium oxide post-treated by nitrogen rapid thermal annealing. Journal of Vacuum Science and Technology B:Nanotechnology and Microelectronics, 2014, 32, 03D113.	1.2	8
41	Light-Immune pH Sensor with SiC-Based Electrolyte–Insulator–Semiconductor Structure. Applied Physics Express, 2013, 6, 127002.	2.4	7
42	Thin-film light-addressable potentiometric sensor with SnOx as a photosensitive semiconductor. Vacuum, 2019, 168, 108809.	3.5	7
43	Fluorographene sensing membrane in a light-addressable potentiometric sensor. Ceramics International, 2019, 45, 9074-9081.	4.8	7
44	Effects of CF4Plasma Treatment on pH and pNa Sensing Properties of Light-Addressable Potentiometric Sensor with a 2-nm-Thick Sensitive HfO2Layer Grown by Atomic Layer Deposition. Japanese Journal of Applied Physics, 2011, 50, 04DL06.	1.5	7
45	Effects of CF ₄ Plasma Treatment on pH and pNa Sensing Properties of Light-Addressable Potentiometric Sensor with a 2-nm-Thick Sensitive HfO ₂ Layer Grown by Atomic Layer Deposition. Japanese Journal of Applied Physics, 2011, 50, 04DL06.	1.5	6
46	The effect of operating conditions on the optically induced electrokinetic (OEK)-based manipulation of magnetic microbeads in a microfluidic system. Sensors and Actuators B: Chemical, 2019, 296, 126610.	7.8	6
47	Gold Nanoframe Array Electrode for Straightforward Detection of Hydrogen Peroxide. Chemosensors, 2021, 9, 37.	3.6	6
48	Optimization of a PVC Membrane for Reference Field Effect Transistors. Sensors, 2009, 9, 2076-2087.	3.8	5
49	Fluorine Incorporation and Thermal Treatment on Single and Stacked Si[sub 3]N[sub 4] Membranes for ISFET/REFET Application. Journal of the Electrochemical Society, 2010, 157, J8.	2.9	5
50	Nano-IGZO layer for EGFET in pH sensing characteristics. , 2013, , .		5
51	The Effect of Monolayer Graphene on the UV Assisted NO2 Sensing and Recovery at Room Temperature. Proceedings (mdpi), 2017, 1, .	0.2	5
52	Sensitivity of Trapping Effect on Si ₃ N ₄ Sensing Membrane for Ion Sensitive Field Effect Transistor/Reference Field Effect Transistor Pair Application. Sensor Letters, 2010, 8, 725-729.	0.4	5
53	Sodium and potassium ion sensing properties of EIS and ISFET structures with fluorinated hafnium oxide sensing film. , 2009, , .		4
54	Effects of Thickness Effect and Rapid Thermal Annealing on pH Sensing Characteristics of Thin HfO ₂ Films Formed by Atomic Layer Deposition. Japanese Journal of Applied Physics, 2011, 50, 10PG03.	1.5	4

#	Article	IF	CITATIONS
55	Effects of Thickness Effect and Rapid Thermal Annealing on pH Sensing Characteristics of Thin HfO\$_{2}\$ Films Formed by Atomic Layer Deposition. Japanese Journal of Applied Physics, 2011, 50, 10PG03.	1.5	3
56	VERTICAL SILICON NANOWIRES WITH ATOMIC LAYER DEPOSITION WITH HfO₂ MEMBRANE FOR pH SENSING APPLICATION. Journal of Mechanics in Medicine and Biology, 2011, 11, 959-966.	0.7	3
57	DRAM Data Retention and Cell Transistor Threshold Voltage Reliability Improved by Passivation Annealing Prior to the Deposition of Plasma Nitride Layer. IEEE Transactions on Device and Materials Reliability, 2012, 12, 406-412.	2.0	3
58	P-I-N Amorphous Silicon Light-Addressable Potentiometric Sensors for High-photovoltage Chemical Image. Procedia Engineering, 2015, 120, 1015-1018.	1.2	3
59	Nitrogen ratio and RTA optimization on sputtered TiN/SiO2/Si electrolyte-insulator–semiconductor structure for pH sensing characteristics. Vacuum, 2015, 118, 113-117.	3.5	3
60	Capacitive Sweat Sensor Constructed by Gui Diatomaceous Earth. Procedia Engineering, 2016, 168, 181-184.	1.2	3
61	Programming a nonvolatile memory-like sensor for KRAS gene sensing and signal enhancement. Biosensors and Bioelectronics, 2016, 79, 63-70.	10.1	3
62	Scanning Spreading Resistance Microscopy for Doping Profile in Saddle-Fin Devices. IEEE Nanotechnology Magazine, 2017, 16, 999-1003.	2.0	3
63	An integrated actuating and sensing system for light-addressable potentiometric sensor (LAPS) and light-actuated AC electroosmosis (LACE) operation. Biomicrofluidics, 2021, 15, 024109.	2.4	3
64	pH Sensing Characterization of Programmable Sm2O3/Si3N4/SiO2/Si Electrolyte–Insulator–Semiconductor Sensor with Rapid Thermal Annealing. Japanese Journal of Applied Physics, 2011, 50, 10PCO4.	1.5	3
65	Laser Illumination Adjustments for Signal-to-Noise Ratio and Spatial Resolution Enhancement in Static 2D Chemical Images of NbOx/IGZO/ITO/Glass Light-Addressable Potentiometric Sensors. Chemosensors, 2021, 9, 313.	3.6	3
66	Differential Light Addressable Potentiometric Sensor with Poly(vinyl chloride) and HfO2Membranes for pH Sensors. Japanese Journal of Applied Physics, 2010, 49, 04DL10.	1.5	2
67	Ultra-high scanning speed chemical image sensor based on light addressable potentiometric sensor with analog micro-mirror. , 2013, , .		2
68	A IGZO-based light-addressable potentiometric sensor on a PET susbtrate. , 2019, , .		2
69	A Systematic Study and Potential Limitations of Proton-ELISA Platform for α-Synuclein Antigen Detection. Chemosensors, 2022, 10, 5.	3.6	2
70	Nanohollow Titanium Oxide Structures on Ti/FTO Glass Formed by Step-Bias Anodic Oxidation for Photoelectrochemical Enhancement. Nanomaterials, 2022, 12, 1925.	4.1	2
71	The characterization of stacked α-Si/SiGe/α-Si sensing membrane. Microelectronic Engineering, 2005, 80, 46-49.	2.4	1
72	Chemical Sensing Properties of Electrolyte/SiGe/SiO2/Si Structure. Japanese Journal of Applied Physics, 2006. 45. 6192-6195.	1.5	1

#	Article	IF	CITATIONS
73	Residual Clamping Force and Dynamic Random Access Memory Data Retention Improved by Gate Tungsten Etch Dechucking Condition in a Bipolar Electrostatic Chuck. Japanese Journal of Applied Physics, 2012, 51, 086502.	1.5	1
74	Dependence of DRAM Device Performance on Passivation Annealing Position in Trench and Stack Structures for Manufacturing Optimization. IEEE Transactions on Semiconductor Manufacturing, 2012, 25, 657-663.	1.7	1
75	Real-time 2D pH images by fast scanning light-addressable Potentiometrie sensor system controlled by LabVIEW program. , 2015, , .		1
76	Thin silicon light-addressable potentiometric sensor by Deep reactive-ion etching. , 2017, , .		1
77	Characterization on pH Sensing and Corrosion-Resistant of HfTaO Membrane with Post RTA Treatment for Food Industry. Sensor Letters, 2010, 8, 720-724.	0.4	1
78	Reference Electrode–Insulator–Nitride–Oxide–Semiconductor Structure with Sm2O3Sensing Membrane for pH-Sensor Application. Japanese Journal of Applied Physics, 2011, 50, 04DL09.	1.5	1
79	The surface site dehydration mechanism for Si/sub 3/N/sub 4/ sensing membrane by post-baking treatment. , 2004, , .		0
80	Nitrogen effects on the sensitivity of tantalum nitride (Ta/sub x/N) for ion sensing devices. , 2004, , .		0
81	Ion sensing improvements of hafnium oxide by nitrogen incorporation. , 2004, , .		0
82	Sensitivity improvements of Hf <inf>x</inf> W <inf>y</inf> O <inf>z</inf> sensing membranes for pK sensors based on electrolyte-insulator-semiconductor structure. , 2009, , .		0
83	Single Si <inf>3</inf> N <inf>4</inf> layer on dual substrate for pH sensing micro sensor. , 2009, , .		0
84	pH Sensing Characterization of Programmable Sm\$_{2}\$O\$_{3}\$/Si\$_{3}\$N\$_{4}\$/SiO\$_{2}\$/Si Electrolyte–Insulator–Semiconductor Sensor with Rapid Thermal Annealing. Japanese Journal of Applied Physics, 2011, 50, 10PG04.	1.5	0
85	Reference Electrode–Insulator–Nitride–Oxide–Semiconductor Structure with Sm2O3Sensing Membrane for pH-Sensor Application. Japanese Journal of Applied Physics, 2011, 50, 04DL09.	1.5	0
86	Functionalization of nanoscaled 2 nm-thick ALD-HfO <inf>2</inf> layer by rapid thermal annealing and CF <inf>4</inf> plasma for LAPS NH <inf>4</inf> ⁺ detection. , 2011, , .		0
87	Highly sensitivity of potassium ion detection realized on fluorinated-HfO <inf>2</inf> by fluorine implantation on EIS. , 2011, , .		0
88	In-Line Supermapping of Storage Capacitor for Advanced Stack DRAM Reliability. IEEE Transactions on Device and Materials Reliability, 2013, 13, 66-72.	2.0	0
89	Negative Bias Temperature Instability for Sputtering Modification in a TiN Diffusion Barrier of p+ Polysilicon Gate Stack in 50-nm DRAM Technology. IEEE Transactions on Device and Materials Reliability, 2013, 13, 81-86.	2.0	0
90	Extended titanium nitride gate field-effect transistor with PVC selective membrane for hydrogen and potassium ion detection. , 2014, , .		0

#	Article	IF	CITATIONS
91	High photocurrent and operation frequency for light-addressable potentiometric sensor by thinner Si substrate. , 2014, , .		0
92	High photocurrent and high frequency response of light-addressable potentiometrie sensor with thin Si substrate and surface roughness. , 2015, , .		0
93	Self-assembly La-rich nanocrystals in metal-gate MIS structures for non-volatile memories. Microelectronic Engineering, 2015, 138, 27-30.	2.4	0
94	Thickness effect of IGZO layer in light-addressable potentiometric sensor. , 2016, , .		0
95	C3A Epithelium Cells Directly Cultured on High-Dielectric Constant Material for Light-Addressable Potentiometric Sensor. Proceedings (mdpi), 2018, 2, 1021.	0.2	0
96	Magnetic Beads Actuating and Sensing by Light Addressability. Proceedings (mdpi), 2018, 2, .	0.2	0
97	A Multi-Well Thin-Si LAPS and All-in-One Readout System for Ion Activity Monitor of Epithelium Cells. Proceedings (mdpi), 2018, 2, .	0.2	0